

Demonstration of $K^0\bar{K}^0$, $B^0\bar{B}^0$, and $D^0\bar{D}^0$ Transitions with a Pair of Coupled Pendula

Klaus R. Schubert

Institut für Kern- und Teilchenphysik, Technische Universität Dresden

and Jürgen Stiewe

Kirchhoff-Institut für Physik, Universität Heidelberg

Abstract: A setup of two coupled and damped pendula is used to demonstrate the main features of transitions between the neutral mesons K^0 , D^0 , B^0 and their antiparticles, including CP violation in the K^0 system. The transitions are described by two-state Schrödinger equations. Since the real parts of their solutions obey the same differential equations as the pendula coordinates, the pendulum motions can be used to represent the meson transitions. Video clips of the motions are attached as supplementary material.

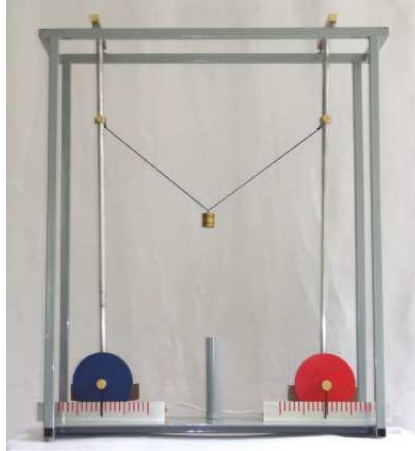


Figure 1: Photograph of the demonstration pendula.

1. Introduction

We describe two coupled pendula which we built, inspired by a presentation of B. Winstein [1], in 1987 when transitions between B^0 and \bar{B}^0 mesons had been discovered [2]. Since then, the pendula have been presented many times for visualizing the evolution of states $\psi_1 M^0 + \psi_2 \bar{M}^0$ where M^0 is a K^0 , D^0 , or B^0 meson, and \bar{M}^0 is its respective antiparticle. A meson is an elementary particle consisting of one quark and one antiquark. It, therefore, belongs neither to matter nor to antimatter. Some mesons are their own antiparticle like the photon, an example is the neutral π -meson π^0 . The K^0 meson and its antiparticle \bar{K}^0 are different particles, they differ in their properties and their quark content. The

phenomenon that a K^0 may transform itself spontaneously into a \bar{K}^0 , called $K^0\bar{K}^0$ transition, is a non-trivial but now well-understood consequence of the weak interaction. In a world with six quark flavors, where one quark (top) is so heavy that it decays before it can form a meson, the above-mentioned $M^0\bar{M}^0$ pairs and $B_s\bar{B}_s$ are the only four which show transitions $M^0 \leftrightarrow \bar{M}^0$. All four transition types have been observed in experiments at particle accelerators.

In these experiments studies of the discrete symmetries under the operations C, P, CP, T, and CPT have played an important role, where C denotes the exchange of particles and antiparticles like $K^0 \rightarrow \bar{K}^0$, P the parity operation $\vec{r} \rightarrow -\vec{r}$, and T the time-reversal operation ($t \rightarrow -t$ and exchanging ingoing and outgoing states).

Table 1: Transition parameters and properties of the four two-state systems $M^0\bar{M}^0$ [7, 8]. The parameters in the first five lines are defined in the text. The parameter $|p/q|$ describes CP violation in the transitions. If no error is given, the precision of the parameter is higher than the number of digits given. The last line gives the property combinations of the two fundamental states for each system. These states are Long (L)- or Short (S)-living, heavy (h) or light (ℓ), CP-even (+) or CP-odd (-); there are no first-principle relations between the three properties.

	$K^0\bar{K}^0$	$D^0\bar{D}^0$	$B^0\bar{B}^0$	$B_s\bar{B}_s$
μ [MeV]	498	1865	5279	5366
Γ [s^{-1}]	$5.59 \cdot 10^9$	$2.44 \cdot 10^{12}$	$6.6 \cdot 10^{11}$	$6.8 \cdot 10^{11}$
$ \Delta m $ [s^{-1}]	$5.3 \cdot 10^9$	$(1.5 \pm 0.5) \cdot 10^{10}$	$5.1 \cdot 10^{11}$	$1.8 \cdot 10^{13}$
$\Delta\Gamma$ [s^{-1}]	$1.115 \cdot 10^{10}$	$(3.9 \pm 0.6) \cdot 10^{10}$	$< 3 \cdot 10^{10}$	$(6 \pm 2) \cdot 10^{10}$
χ	0.4986	$(5.1 \pm 1.6) \cdot 10^{-5}$	0.19	0.4993
$ p/q - 1$	$3.3 \cdot 10^{-3}$	0.1 ± 0.2	$(-2.4 \pm 2.3) \cdot 10^{-3}$	$(-4 \pm 3) \cdot 10^{-3}$
	$\ell = + = S$	$h = + = S$	$h = ? = ?$	$? = + = S$

Transitions between K^0 and \bar{K}^0 mesons were predicted by M. Gell-Mann and A. Pais [3] in 1955. First observations 1958 in nuclear emulsion [4] and in a hydrogen bubble chamber [5] were based on the appearance of \bar{K}^0 mesons in a K^0 beam. These and all later $K^0\bar{K}^0$ observations are successfully described by a two-state Schrödinger equation. Many superpositions $\psi_1 K^0 + \psi_2 \bar{K}^0$ are solutions of the equation, but only two of them have an exponential decay law. They are called K^0_S with a decay rate Γ_S and K^0_L with $\Gamma_L \ll \Gamma_S$. These states have also different masses, m_S and m_L respectively. Because of (weakly broken) CP symmetry, the states are also (approximate) CP eigenstates; $CP(K^0_S) = +1$ and $CP(K^0_L) = -1$. The latest experimental results for $\mu = (m_S + m_L)/2$, $\Delta m = m_S - m_L$, $\Gamma = (\Gamma_S + \Gamma_L)/2$, and $\Delta\Gamma = \Gamma_S - \Gamma_L$ are given in Table 1. The transition strength is given

by the parameter $\chi(M^0)$,

$$\chi(M^0) = \text{fraction of all } M^0 \text{ decaying as } \overline{M}^0 = \frac{4(\Delta m)^2 + (\Delta\Gamma)^2}{8\Gamma^2 + 8(\Delta m)^2}, \quad \chi(K^0) = 0.4986. \quad (1)$$

$B^0\overline{B}^0$ transitions were first observed 1987 at DESY [2]. Present values for μ , Δm , and Γ are given in Table 1; for $\Delta\Gamma$ we have only an upper limit, and

$$\chi(B^0) = 0.19. \quad (2)$$

First evidence for $B_s\overline{B}_s$ transitions, more precisely for the sum of $B_s \leftrightarrow \overline{B}_s$ and $B^0 \leftrightarrow \overline{B}^0$, was reported by the UA1 group [9] in 1987. A significant determination of $\Delta m(B_s)$, however, could be reached only in 2006 at Fermilab [10, 11]; we now know that

$$\chi(B_s) = 0.4993. \quad (3)$$

$D^0\overline{D}^0$ transitions were discovered in 2007 by the experiments BABAR [12] and BELLE [13]. Additional data in the last four years lead to the results in Table 1, and

$$\chi(D^0) = 5 \cdot 10^{-5}. \quad (4)$$

The study of $M^0\overline{M}^0$ transitions has played an important role in the progress of particle physics, especially in understanding the weak interaction. A summary would be beyond the scope of our article, we only mention the 1964 discovery of CP-symmetry breaking in $K^0\overline{K}^0$ transitions [14] leading to the Physics Nobel Prize in 1980. The mere observation that Δm , Γ , and $\Delta\Gamma$ are very small compared to μ for each meson pair shows that the transitions are produced by weak interactions. This ensures two relevant facts: First, the evolution of the states $\Psi = (\psi_1, \psi_2)$ for each pair is given by a linear differential equation, the Schrödinger equation $i \partial\Psi/\partial t = \mathbf{M} \Psi$ with a 2×2 complex matrix \mathbf{M} ; each pair has a different set of eight real constants in \mathbf{M} . Second, the real parts $\Re(\psi_1)$ and $\Re(\psi_2)$ contain the same information as the complex solutions Ψ . The latter is the basis for the main concern of the article: The evolutions of $M^0\overline{M}^0$ transitions may be represented by motions of coupled pendula.

Owing to arbitrary phases of the states M^0 and \overline{M}^0 , only seven of the eight constants in \mathbf{M} have a physical meaning. The most general solution Ψ has seven parameters which follow unambiguously from the seven constants in \mathbf{M} . Discrete symmetries reduce the number of constants and parameters [15]; CPT symmetry leaves five, T symmetry leaves six, and the combination of CPT and T, which also means CP symmetry, leaves four. In Section 4, we discuss the most general CP-symmetric equation and its solutions, in Appendix 2 the most general CPT-symmetric case. The motions of our coupled pendula represent the real parts of Ψ , they obey the same differential equations as the deflection angles ϕ_1 and ϕ_2 of the pendula. The pendula are described in Section 2. In Sections 3 and 4, we discuss the Schrödinger-equation solutions for a stable particle, a decaying particle, and a quasi-stable two-particle system, corresponding to the motions of an undamped pendulum, a damped

pendulum, and a pair of coupled but undamped pendula, respectively.

The motions are shown in a series of video clips which are attached as supplementary material [6]. In Section 5, we discuss the most general CP-symmetric two-state Schrödinger equation and the corresponding equations of motion. In Section 6, we present $K^0\bar{K}^0$, $B^0\bar{B}^0$, and $D^0\bar{D}^0$ transitions with the same pendulum setup by translating the three parameter sets in \mathbf{M} into the corresponding parameters for coupling and damping the pendula. In Section 7 we discuss CP-symmetry breaking in transitions $K^0 \leftrightarrow \bar{K}^0$. We choose an asymmetric pendulum setup for demonstrating the main feature of this CP violation, $K_L^0 = p K^0 + q \bar{K}^0$ with $|p/q| > 1$. However, the presented setup has an equation of motion which does not correspond to a CPT-symmetric and T-violating Schrödinger equation.

2. Description of the Pendulum Pair

Fig. 1 shows a photograph of our setup. The two mechanically identical pendula, differing only by colour, are suspended in a steel housing and can swing freely, nearly frictionless. The coupling between the pendula is established through a thin thread which connects the pendulum rods and can carry weights of different magnitudes as to strengthen or loosen the coupling. Also the length of the thread and its connection points to the rods are adjustable. Each pendulum carries a copper sheet which can slide in the opening of an electromagnet in order to introduce individual damping by exciting eddy currents in the copper sheets. Damping in the coupling is also possible, see below. A technical drawing of steel housing and pendula, including the major measures, is shown in Fig. 2. Detailed construction drawings with all measures and a 3D drawing are available in the supplementary material [6].

The frame which houses the pendula is made of steel tubes with a square cross section, the ground plate consists of an aluminium sheet. The two long tubes on the upper side of the frame carry two half-globular pits with 15 mm diameter, made of case-hardened steel. The pits serve as abutments for the steel pins on the pendula, see below. The distance between the two pendula is 500 mm. For measuring the amplitudes of the pendula, two scales with spacings of 1 cm each are attached to the ground plate in variable positions.

Each of the two pendula consists of a round aluminium rod on the upper side of which a brass traverse bar is fixed giving the upper side of the pendulum a T-shaped appearance. Below the traverse bar, two pins of case-hardened steel are fixed fitting into the above-mentioned steel pits. Their tips represent the centres of the pendulum movements. The rotation axes of the pendula are defined by the points where the pins touch the pits. The pendulum bobs are thin circular aluminium plates screwed to the pendulum rods whose distances ℓ from the pendulum axes can be varied; for the demonstrations we use $\ell = 710$ mm. Each plate carries on its back a brass weight of 0.6 kg adapted to the plate shape.

The two ends of the thread connecting the pendula can be fixed at the pendulum rods at

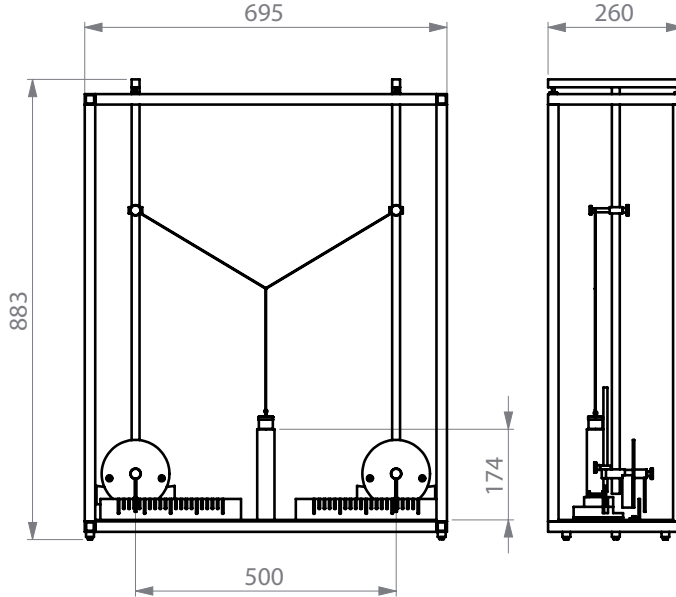


Figure 2: Pendula and frame with major measures in mm.

different distances from the rotation axes so that different lever arms can be chosen. In our standard demonstration, corresponding to the attached video clips, the thread is 100 mm longer than the pendulum distance, the two lever arms are 180 mm long, and the weights are 150, 250, and 12 grams for $\overline{K\overline{K}}$, $\overline{B\overline{B}}$, and $\overline{D\overline{D}}$ transitions, respectively.

Screwed to the lower end of each pendulum rod is a brass bar of circular cross section with a copper sheet soldered to its lower end. The copper sheet is 3 mm thick and has the shape of a circle segment following the pendulum bob's oscillation trajectory. It fits in the opening of an electromagnet fixed to the aluminium ground plate of the pendulum frame. The coil is driven by an AC voltage of $U_{\text{eff}} = 18 \text{ V}$ and produces a field with an amplitude of 0.10 Tesla exciting eddy currents in the copper sheet which damp the oscillation of each pendulum separately.

Damping in the coupling - a salient point - is realized in the following way: The brass weight which is used to establish the coupling between the pendula in the $\overline{K\overline{K}}$ demonstrations (Pos. 38 in the construction drawings [6]) can be suspended on a separate thread such that it can dive into a brass cylinder which is fixed vertically to the ground plate. The inner diameter of the cylinder corresponds to the weight's diameter. A narrow bore runs through the brass weight in parallel to its vertical axis. The vertical up- and down movements of the weight, following the pendulum swing, press air through the bore which flows in a laminar way, due to the slow movement. The air flow can be adjusted by a screw rectangular to the bore.

3. Stable and Unstable Particles

Using $\hbar = c = 1$, the Schrödinger equation of a stable particle with mass m in its rest frame is given by

$$i \partial\psi/\partial t = m \cdot \psi , \quad (5)$$

where t is its eigentime. The complex solution,

$$\psi = \Re + i\Im = e^{-imt} , \quad (6)$$

has two components which carry the same information as ψ , the mass m and

$$|\psi|^2 = 2\langle \cos^2 mt \rangle = 2\langle \sin^2 mt \rangle = 1, \quad (7)$$

where $\langle \rangle$ means averaging over times $T \gg 1/m$. With in addition $T \ll 1/\Gamma$ and $T \ll 1/\Delta m$, the property $\langle \Re_i^2 \rangle = |\psi_i|^2/2$, $i = 1, 2$ holds for all cases discussed in this article, as shown in Appendix 1. The real part of ψ obeys

$$\ddot{\Re} = -m^2 \Re . \quad (8)$$

In small-angle approximation, the equation of motion for a mathematical pendulum with length ℓ and acceleration g is the same when $m^2 = g/\ell$. Video01 [6] shows this motion with the oscillation period $2\pi/m = 1.69$ s. The stable particle is represented by the undamped pendulum.

The effective Schrödinger equation of an unstable particle, effective since it does not include the final states into which the particle may decay, is given by

$$i \partial\psi/\partial t = (m - i\Gamma/2) \cdot \psi , \quad (9)$$

where the total decay rate Γ is the sum of the partial rates into all final states. If the particle decays only weakly with $\Gamma \ll m$, Eq. 9 is a very good approximation [16]. Its solution is

$$\psi = \Re + i\Im = e^{-imt} \cdot e^{-\Gamma t/2}, \quad (10)$$

where \Re obeys

$$\ddot{\Re} = -(m^2 + \Gamma^2/4)\Re - \Gamma\dot{\Re} , \quad (11)$$

the equation of motion for a pendulum with velocity-proportional damping. Again ψ and \Re carry the same information, m and

$$|\psi|^2 = 2\langle \Re^2 \rangle = e^{-\Gamma t} . \quad (12)$$

The motion with $1/\Gamma = 7$ s is shown in Vido02 [6]; its frequency is insignificantly smaller than that of the undamped pendulum. The time-averaged amplitude square represents the probability that the particle has not yet decayed.

4. Transitions in a Symmetric Pair of Stable Particles

The next introductory example, two coupled same-length pendula with negligible damping, has no analogy in meson physics but corresponds to the two states of an ammonia molecule as discussed e. g. by R. Feynman [17]. The Schrödinger equation for a two-state system of coupled particles with negligible damping can be written as

$$i \frac{\partial \Psi}{\partial t} = \mathbf{M} \Psi = \begin{pmatrix} m+k & -k \\ -k & m+k \end{pmatrix} \Psi . \quad (13)$$

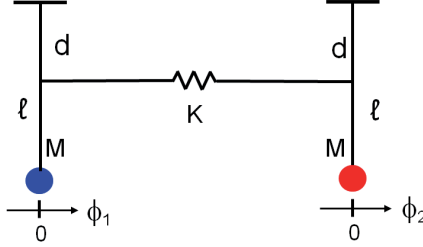


Figure 3: Coupled mathematical pendula without damping; coordinates are the angles ϕ_1 and ϕ_2 , parameters are mass M , pendulum length ℓ , gravitational acceleration g , and the two parameters for the coupling torque, lever arm d and proportionality constant K .

The linear combinations $\psi_1 + \psi_2$ and $\psi_1 - \psi_2$ obey uncoupled equations, leading to

$$(\ddot{\mathfrak{R}}_1 + \ddot{\mathfrak{R}}_2) = -m^2 \cdot (\mathfrak{R}_1 + \mathfrak{R}_2) , \quad (\ddot{\mathfrak{R}}_1 - \ddot{\mathfrak{R}}_2) = -(m+2k)^2 \cdot (\mathfrak{R}_1 - \mathfrak{R}_2) \quad (14)$$

and consequently to

$$\begin{pmatrix} \ddot{\mathfrak{R}}_1 \\ \ddot{\mathfrak{R}}_2 \end{pmatrix} = - \begin{pmatrix} m^2 + 2mk + 2k^2 & -2mk - 2k^2 \\ -2mk - 2k^2 & m^2 + 2mk + 2k^2 \end{pmatrix} \begin{pmatrix} \mathfrak{R}_1 \\ \mathfrak{R}_2 \end{pmatrix} \quad (15)$$

for the real parts \mathfrak{R}_1 and \mathfrak{R}_2 of ψ_1 and ψ_2 . Our mechanical analogon is the pendulum pair in Fig. 3. For the left-side pendulum, the coupling force is $F_{12} = -K(d \cdot \phi_1 - d \cdot \phi_2)$, for the other one $F_{21} = -F_{12}$, and the torques are $F_{ij} \cdot d$. The equation of rotary motion is

$$M\ell^2 \begin{pmatrix} \ddot{\phi}_1 \\ \ddot{\phi}_2 \end{pmatrix} = - \begin{pmatrix} Mg\ell + Kd^2 & -Kd^2 \\ -Kd^2 & Mg\ell + Kd^2 \end{pmatrix} \begin{pmatrix} \phi_1 \\ \phi_2 \end{pmatrix} . \quad (16)$$

The differential equations in Eqs. 15 and 16 are identical when $m^2 = g/\ell$ and $2mk + 2k^2 = Kd^2/(M\ell^2)$, i. e. these pendula motions represent undamped transitions between two quantum-mechanical states. With $\phi_i = \mathfrak{R}_i$ the solutions of Eqs. 14 are

$$\phi_1 + \phi_2 = \alpha \cdot \cos(mt - \beta) , \quad \phi_1 - \phi_2 = \gamma \cdot \cos[(m+2k)t - \delta] , \quad (17)$$

and their sum is the most general pendulum motion with four adjustable parameters to be fixed by the conditions at $t = 0$. We now show four special solutions:

i) The parallel fundamental mode in Video03 [6] with $\gamma = \beta = 0$,

$$\phi_1 = \phi_2 = \phi_0 \cdot \cos mt . \quad (18)$$

ii) The antiparallel fundamental mode in Video04 [6] with $\alpha = \delta = 0$,

$$\phi_1 = -\phi_2 = \phi_0 \cdot \cos(m + 2k)t . \quad (19)$$

Its frequency is larger than in case (i); the “mass difference” $2k$ is given by the matrix element M_{12} in Eq. 13. The initial conditions for modes i) and ii) are the only ones which lead to time-independent amplitudes for ϕ_1 and ϕ_2 . All other conditions lead to oscillation modes with beats, i. e. with varying amplitudes.

iii) “Blue starts and Red is at rest” in Video05 [6] with $\phi_1(0) = \phi_0$, $\phi_2(0) = \dot{\phi}_1(0) = \dot{\phi}_2(0) = 0$ leading to

$$\begin{aligned} \phi_1(t) &= \phi_0 \cdot [\cos(\mu - k)t + \cos(\mu + k)t]/2 = \phi_0 \cdot \cos kt \cdot \cos \mu t , \\ \phi_2(t) &= \phi_0 \cdot [\cos(\mu - k)t - \cos(\mu + k)t]/2 = \phi_0 \cdot \sin kt \cdot \sin \mu t , \end{aligned} \quad (20)$$

where $\mu = m + k$. Our demonstration shows the oscillation period in between that of modes i) and ii) and the beat period of $2\pi/k = 57$ s.

iv) “Red starts and Blue is at rest” in Video06 [6] with $\phi_2(0) = \phi_0$, $\phi_1(0) = \dot{\phi}_1(0) = \dot{\phi}_2(0) = 0$, leading to $\phi_1(t) = \phi_2$ of motion (iii) and $\phi_2(t) = \phi_1$ of motion (iii). The two motions are perfect mirror images of each other; this symmetry corresponds to CP symmetry in the meson transitions.

5. Transitions in a CP-Symmetric Meson Pair

The most general Schrödinger equation for the evolution of the state $\psi_1 M^0 + \psi_2 \bar{M}^0$ including transitions between M^0 and \bar{M}^0 is

$$i \frac{\partial}{\partial t} \begin{pmatrix} \psi_1 \\ \psi_2 \end{pmatrix} = \left[\begin{pmatrix} m_{11} & m_{12} \\ m_{12}^* & m_{22} \end{pmatrix} - \frac{i}{2} \begin{pmatrix} \Gamma_{11} & \Gamma_{12} \\ \Gamma_{12}^* & \Gamma_{22} \end{pmatrix} \right] \begin{pmatrix} \psi_1 \\ \psi_2 \end{pmatrix} , \quad (21)$$

where m_{11} , m_{22} , Γ_{11} , Γ_{22} are real and m_{12} , Γ_{12} are complex. The equation was derived from perturbation theory in 1930 [18] and in a stricter way from field theory in 1963 [19]. A comprehensive treatment of all its properties and symmetries can be found in [15]. The phases of m_{12} and Γ_{12} are arbitrary, but their relative phase ξ is an observable. CPT invariance requires $m_{11} = m_{22}$ and $\Gamma_{11} = \Gamma_{22}$. T symmetry requires $\xi = 0$ or π , i. e. m_{12} and Γ_{12} can be chosen to be real. CP symmetry requires both CPT and T symmetry; we write the CP-symmetric equation as

$$i \frac{\partial}{\partial t} \begin{pmatrix} \psi_1 \\ \psi_2 \end{pmatrix} = \left[\begin{pmatrix} \mu & m_{12} \\ m_{12} & \mu \end{pmatrix} - \frac{i}{2} \begin{pmatrix} \Gamma & \Gamma_{12} \\ \Gamma_{12} & \Gamma \end{pmatrix} \right] \begin{pmatrix} \psi_1 \\ \psi_2 \end{pmatrix} , \quad (22)$$

with four real parameters. Its two fundamental solutions are

$$\begin{aligned} \psi_1 + \psi_2 &= e^{-(\Gamma+\Gamma_{12})t/2} e^{-i(\mu+m_{12})t} , \quad \psi_1 - \psi_2 = 0 , \\ \text{and } \psi_1 - \psi_2 &= e^{-(\Gamma-\Gamma_{12})t/2} e^{-i(\mu-m_{12})t} , \quad \psi_1 + \psi_2 = 0 . \end{aligned} \quad (23)$$

The rate Γ is determined by the sum of all decays of the M^0 . The rate $|\Gamma_{12}|$, necessarily smaller than Γ , is determined by all those final states which are reached from both M^0 and \bar{M}^0 , examples are $\pi^+\pi^-$ and $\pi^0\pi^0$ in the $K^0\bar{K}^0$ system.

K and B mesons differ strongly in their ratio Γ_{12}/Γ . For the Kaons, the sum of $\pi^+\pi^-$ and $\pi^0\pi^0$ dominates all decays; $|\Gamma_{12}| = \Gamma$ in good approximation. We choose the unobservable sign of Γ_{12} to be negative,

$$\Gamma(K) + \Gamma_{12}(K) \approx 0 , \quad \Gamma(K) - \Gamma_{12}(K) \approx 2\Gamma(K) , \quad (24)$$

and $\psi_1 - \psi_2$ in Eq. 23 describes the K^0_S , $\psi_1 + \psi_2$ the K^0_L . In the B-meson system, Γ is dominated by those final states which are reached from either only B^0 or only \bar{B}^0 . In contrast to $|\Gamma_{12}(K)/\Gamma(K)| \approx 1$, we have $|\Gamma_{12}(B)/\Gamma(B)| \ll 1$ and for the demonstration we can approximate $\Gamma_{12}(B) = 0$. For the D-meson pair we have $|\Gamma_{12}(D)/\Gamma(D)| \ll 1$ as well, the distinction is the smallness of $|m_{12}(D)|$. The ratio $|m_{12}(D)/\Gamma(D)|$ is of the order 10^{-2} , whereas $|m_{12}(B)/\Gamma(B)| = o(1)$.

Setting $m_{12} = -k$, $\mu + m_{12} = m$ and using the above approximations for Γ_{12} , we obtain for the K mesons

$$\begin{aligned} \begin{pmatrix} \ddot{\mathfrak{R}}_1 \\ \ddot{\mathfrak{R}}_2 \end{pmatrix} &= - \begin{pmatrix} m^2 + 2mk + 2k^2 + \Gamma^2/2 & -2mk - 2k^2 - \Gamma^2/2 \\ -2mk - 2k^2 - \Gamma^2/2 & m^2 + 2mk + 2k^2 + \Gamma^2/2 \end{pmatrix} \begin{pmatrix} \mathfrak{R}_1 \\ \mathfrak{R}_2 \end{pmatrix} \\ &\quad - \begin{pmatrix} \Gamma & -\Gamma \\ -\Gamma & \Gamma \end{pmatrix} \begin{pmatrix} \dot{\mathfrak{R}}_1 \\ \dot{\mathfrak{R}}_2 \end{pmatrix} , \end{aligned} \quad (25)$$

and for the B and D mesons

$$\begin{aligned} \begin{pmatrix} \ddot{\mathfrak{R}}_1 \\ \ddot{\mathfrak{R}}_2 \end{pmatrix} &= - \begin{pmatrix} m^2 + \Gamma^2/4 + 2mk + 2k^2 & -2mk - 2k^2 \\ -2mk - 2k^2 & m^2 + \Gamma^2/4 + 2mk + 2k^2 \end{pmatrix} \begin{pmatrix} \mathfrak{R}_1 \\ \mathfrak{R}_2 \end{pmatrix} \\ &\quad - \begin{pmatrix} \Gamma & 0 \\ 0 & \Gamma \end{pmatrix} \begin{pmatrix} \dot{\mathfrak{R}}_1 \\ \dot{\mathfrak{R}}_2 \end{pmatrix} . \end{aligned} \quad (26)$$

We now continue with the equations for the corresponding motions of the pendula.

6. Pendulum Motions demonstrating the three Transitions $M^0 \leftrightarrow \bar{M}^0$

The velocity-proportional dampings applied to the pendula are shown in Figs. 4 and 5. For the K system, the coupling force is

$$F_{12} = -F_{21} = -Kd(\phi_1 - \phi_2) - Ad(\dot{\phi}_1 - \dot{\phi}_2) \quad (27)$$

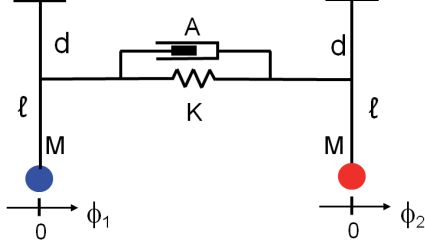


Figure 4: “ $K^0\bar{K}^0$ pendula” with damping in the coupling. A is the proportionality constant between F_{12} and $d \cdot (\dot{\phi}_2 - \dot{\phi}_1)$, the other notations are the same as in Fig. 3.

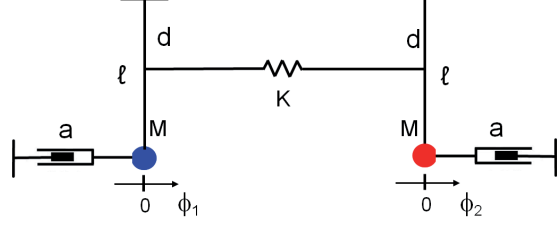


Figure 5: “ $B^0\bar{B}^0$ and $D^0\bar{D}^0$ pendula” with separate dampings for each pendulum. The constant a is the proportionality between damping force and $\ell \cdot \dot{\phi}_i$.

and the equation of motion becomes

$$M\ell^2 \begin{pmatrix} \ddot{\phi}_1 \\ \ddot{\phi}_2 \end{pmatrix} = - \begin{pmatrix} Mg\ell + Kd^2 & -Kd^2 \\ -Kd^2 & Mg\ell + Kd^2 \end{pmatrix} \begin{pmatrix} \phi_1 \\ \phi_2 \end{pmatrix} - \begin{pmatrix} Ad^2 & -Ad^2 \\ -Ad^2 & Ad^2 \end{pmatrix} \begin{pmatrix} \dot{\phi}_1 \\ \dot{\phi}_2 \end{pmatrix}. \quad (28)$$

With $\Gamma = Ad^2/(M\ell^2)$ this is in agreement with Eq. 25. Video07 [6] shows the undamped parallel fundamental solution of Eq. 28 representing the state K^0_L , Video08 [6] the damped antiparallel motion representing the K^0_S . In our setup, the damping time $1/2\Gamma$ is 7 s. If we start the movement with the state \bar{K}^0 , see Video09 [6], its K^0_S component is damped away quickly; at large times we observe only its undamped component K^0_L . A completely symmetric movement is seen in Video10 [6] when we start with the right-side pendulum K^0 .

For demonstrating $B^0\bar{B}^0$ transitions, we change the setup according to Fig. 5 by removing the damping in the coupling and using the two eddy-current brakes of equal strength. The damping forces are now $-a\ell\dot{\phi}_i$ ($i=1,2$), the damping torques $-a\ell^2\dot{\phi}_i$, and the equation of motion is

$$M\ell^2 \begin{pmatrix} \ddot{\phi}_1 \\ \ddot{\phi}_2 \end{pmatrix} = - \begin{pmatrix} Mg\ell + Kd^2 & -Kd^2 \\ -Kd^2 & Mg\ell + Kd^2 \end{pmatrix} \begin{pmatrix} \phi_1 \\ \phi_2 \end{pmatrix} - \begin{pmatrix} a\ell^2 & 0 \\ 0 & a\ell^2 \end{pmatrix} \begin{pmatrix} \dot{\phi}_1 \\ \dot{\phi}_2 \end{pmatrix}. \quad (29)$$

Video11 [6] and Video12 [6] show the fundamental modes; both have the same lifetime, equal to that of the blue and the red mode. In Video13 [6] and Video14 [6], where we start the motion with the blue and the red pendulum respectively, we show the time evolution of the $B^0\bar{B}^0$ transitions. Coupling and dampings are chosen in such a way that the observed transition strength $\chi(B) = 0.19$ is approximated.

For demonstrating $D^0\bar{D}^0$ transitions, we change only the coupling weight and keep the same individual dampings for the two pendula. The lifetimes $1/\Gamma(D)$ and $1/\Gamma(B)$ are

of the same order, but the coupling $|m_{12}(\text{D})|$ is two orders of magnitude smaller than $|m_{12}(\text{B})|$. Video15 [6] shows this case with the red pendulum starting. Its motion is nearly damped away before there is a visible transition of motion energy from the red to the blue side.

7. CP Violation in $\text{K}^0\bar{\text{K}}^0$ Transitions

As shown in Eq. 23, CP symmetry in $\text{K}^0\bar{\text{K}}^0$ transitions leads to two fundamental modes with the properties $\psi_1 - \psi_2 = 0$ and $\psi_1 + \psi_2 = 0$, respectively. If the symmetry is broken this is no longer the case, and the mode K^0_{L} which is reached from K^0 or $\bar{\text{K}}^0$ for times $t \gg 1/\Gamma_{\text{S}}$ contains different fractions of K^0 and $\bar{\text{K}}^0$,

$$\text{K}^0_{\text{L}} = p \text{K}^0 + q \bar{\text{K}}^0 \text{ with } |p/q| \neq 1 . \quad (30)$$

The experimental result is $|p/q| = 1.00332 \pm 0.00003$ [7].

For a simulation with the pendula, we use the setup in Fig. 6. The coupling forces have to obey $F_{21} = -F_{12}$, but the torques can be different if we choose two different lever arms $d_1 > d_2$. Using $d_1 = 20.5$ cm, $d_2 = 15.5$ cm, $\ell\phi_1(0) = 10$ cm, and $\ell\phi_2(0) = 0$ we show in Video16 [6] that, after damping the K^0_{S} mode, the amplitude of the red K^0 in the surviving K^0_{L} is larger than that of the blue $\bar{\text{K}}^0$. The former is 5 cm, the latter 4 cm. Video17 [6] shows the same larger amplitude of the K^0 if we start the motion with the other-side pendulum. These two motions in Video16 and Video17 represent the observed CP violation in the K^0_{L} state.

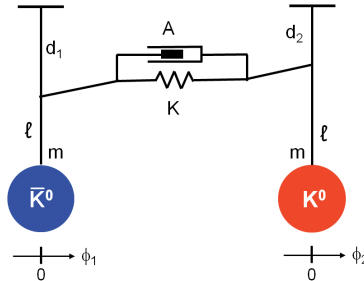


Figure 6: Asymmetric lever arms for the coupling.

The equation of motion for this setup is

$$M\ell^2 \begin{pmatrix} \ddot{\phi}_1 \\ \ddot{\phi}_2 \end{pmatrix} = - \begin{pmatrix} Mg\ell + Kd_1^2 & -Kd_1d_2 \\ -Kd_1d_2 & Mg\ell + Kd_2^2 \end{pmatrix} \begin{pmatrix} \phi_1 \\ \phi_2 \end{pmatrix} - \begin{pmatrix} Ad_1^2 & -Ad_1d_2 \\ -Ad_1d_2 & Ad_2^2 \end{pmatrix} \begin{pmatrix} \dot{\phi}_1 \\ \dot{\phi}_2 \end{pmatrix} . \quad (31)$$

The symmetries of the two matrices (equal off-diagonal and different diagonal elements) are different from those originating from a CPT-symmetric Schrödinger equation, as shown in Appendix 2. $K^0\bar{K}^0$ transitions, however, break both CP and T symmetry and no violation of CPT has been found [20, 21, 22]. In fact, no friction-damped pendulum pair with oscillations in the same space dimension can have an equation of motion originating from a CPT-symmetric and T-violating Schrödinger equation [1, 23]. To our judgement, this should not hinder us to include the present chapter into the article because one of the main features of CP violation in $K^0\bar{K}^0$ transitions is clearly demonstrated.

Examples for coupled and damped oscillations with a CPT-symmetric and T-violating equation of motion are given in the literature; a Foucault pendulum with damping in one direction [24, 25], a ball rolling in a bowl on a turntable [23], and an electrical setup in which the non-reciprocity in the coupling between two resonant circuits is achieved by a gyrator [23, 26]. To our knowledge, none of the proposed demonstration setups has been built so far.

Summary

Starting from two-state Schrödinger equations for pairs of coupled mesons, we derive second-order differential equations for the real parts of their solutions and map them onto equations of motion for a macro-mechanical system. This is a pair of coupled identical pendula with a possible damping in the coupling and individual dampings for each of the pendula. By adjusting the damping and coupling parameters, three different particle-antiparticle transitions and the effect of CP violation can be visualized. The paper is accompanied by a sequence of video clips [6] that demonstrate the performance of the pendula. The case of CPT symmetry along with CP and T violation cannot be reproduced with the setup described. Detailed construction drawings are attached [6] so that the interested reader can build his/her own pendulum pair in order to demonstrate the correspondence between quantum mechanics and macroscopic physics.

Appendix 1. Why does $\text{Re}(\Psi)$ carry the same information as Ψ ?

The most general solution of the linear two-component Schrödinger equation in Eq. 21 is

$$\begin{pmatrix} \psi_1 \\ \psi_2 \end{pmatrix} = a \cdot \begin{pmatrix} p \\ q \end{pmatrix} \cdot e^{-imst} e^{-\Gamma st/2} + b \cdot e^{i\phi} \cdot \begin{pmatrix} r \cdot e^{i\delta} \\ s \end{pmatrix} \cdot e^{-imLt} e^{-\Gamma Lt/2} . \quad (32)$$

With $p^2 + q^2 = 1$ and $r^2 + s^2 = 1$ it contains 10 real parameters, 7 given by the equation $[m = (m_S + m_L)/2, \Delta m = m_S - m_L, \Gamma = (\Gamma_S + \Gamma_L)/2, \Delta\Gamma = \Gamma_S - \Gamma_L, p/q, r/s, \delta]$ and 3 by the initial conditions $[a, b, \phi]$. Without CPT symmetry, $r/s \neq -p/q$ and the phase δ is observable. For the following we also need the weak-interaction conditions $\Gamma \ll m$ and $|\Delta m| \ll m$. The real part of ψ_1 is

$$\Re_1 = a \cdot p \cdot \cos(mt + \Delta m \cdot t/2) e^{-\Gamma st/2} + b \cdot r \cdot \cos(mt - \Delta m \cdot t/2 + \phi + \delta) e^{-\Gamma Lt/2} . \quad (33)$$

With the weak-interaction conditions we obtain

$$\langle \cos^2 m_S t \rangle = \langle \cos^2 m_L t \rangle = \langle \cos^2 m t \rangle = \langle \sin^2 m t \rangle = 1/2 , \quad \langle \cos m t \cdot \sin m t \rangle = 0 , \quad (34)$$

$$2\langle \Re_1^2 \rangle = a^2 p^2 \cdot e^{-\Gamma_S t} + b^2 r^2 \cdot e^{-\Gamma_L t} + 2 abpr \cdot e^{-\Gamma t} \cos(\Delta m \cdot t + \phi + \delta) . \quad (35)$$

The calculation of $|\psi_1|^2$ gives exactly the same result. The conclusion $2\langle \Re_2^2 \rangle = |\psi_2|^2$ is found by just replacing $p \rightarrow q$, $r \rightarrow s$, and $\phi + \delta \rightarrow \phi$.

The equivalence of ψ and $\text{Re}(\psi)$ is far from being general. A simple counter-example is the harmonic oscillator with strong damping. For $\psi = e^{-imt} \cdot e^{-\Gamma t/2}$ with $\Gamma/m = o(1)$ we cannot find averaging intervals with $\langle \text{Re}^2(\psi) \rangle = \langle \text{Im}^2(\psi) \rangle$.

Appendix 2. CPT Symmetry with CP and T Violation

The Schrödinger equation for CPT-conserving but CP- and T-violating $M^0 \bar{M}^0$ transitions is

$$i \frac{\partial}{\partial t} \begin{pmatrix} \psi_1 \\ \psi_2 \end{pmatrix} = \left[\begin{pmatrix} \mu & m_{12} \\ m_{12}^* & \mu \end{pmatrix} - \frac{i}{2} \begin{pmatrix} \Gamma & \Gamma_{12} \\ \Gamma_{12}^* & \Gamma \end{pmatrix} \right] \begin{pmatrix} \psi_1 \\ \psi_2 \end{pmatrix} ; \quad (36)$$

with five observable real parameters, μ , Γ , $|m_{12}|$, $\text{Re}(\Gamma_{12}/m_{12})$, and $\text{Im}(\Gamma_{12}/m_{12})$. Its two fundamental solutions are

$$\begin{pmatrix} \psi_1 \\ \psi_2 \end{pmatrix}_S = \begin{pmatrix} p \\ q \end{pmatrix} \cdot e^{-im_S t} e^{-\Gamma_S t/2} , \quad \begin{pmatrix} \psi_1 \\ \psi_2 \end{pmatrix}_L = \begin{pmatrix} p \\ -q \end{pmatrix} \cdot e^{-im_L t} e^{-\Gamma_L t/2} . \quad (37)$$

The values of the five observables m_S , Γ_S , m_L , Γ_L , and $|p/q|$ follow unambiguously from the five parameters of the Schrödinger equation [15]. The values of p and q can be chosen to be real, leading to

$$\begin{pmatrix} \Re_1 \\ \Re_2 \end{pmatrix}_S = \begin{pmatrix} p \\ q \end{pmatrix} \cdot e^{-\Gamma_S t/2} \cos(m_S t) , \quad \begin{pmatrix} \Re_1 \\ \Re_2 \end{pmatrix}_L = \begin{pmatrix} p \\ -q \end{pmatrix} \cdot e^{-\Gamma_L t/2} \cos(m_L t) . \quad (38)$$

What is the differential equation for the most general superposition,

$$\Re_1 |M^0\rangle + \Re_2 |\bar{M}^0\rangle = \left(\frac{\Re_1}{2p} + \frac{\Re_2}{2q} \right) |M^0_S\rangle + \left(\frac{\Re_1}{2p} - \frac{\Re_2}{2q} \right) |M^0_L\rangle ? \quad (39)$$

The M^0_S and M^0_L components obey the differential equations

$$\begin{aligned} \left(\frac{\ddot{\Re}_1}{2p} + \frac{\ddot{\Re}_2}{2q} \right) &= -(m_S^2 + \Gamma_S^2/4) \left(\frac{\Re_1}{2p} + \frac{\Re_2}{2q} \right) - \Gamma_S \left(\frac{\dot{\Re}_1}{2p} + \frac{\dot{\Re}_2}{2q} \right) , \\ \left(\frac{\ddot{\Re}_1}{2p} - \frac{\ddot{\Re}_2}{2q} \right) &= -(m_L^2 + \Gamma_L^2/4) \left(\frac{\Re_1}{2p} - \frac{\Re_2}{2q} \right) - \Gamma_L \left(\frac{\dot{\Re}_1}{2p} - \frac{\dot{\Re}_2}{2q} \right) , \end{aligned} \quad (40)$$

resulting in

$$\begin{pmatrix} \ddot{\Re}_1 \\ \ddot{\Re}_2 \end{pmatrix} = - \begin{pmatrix} \frac{m_S^2+m_L^2}{2} + \frac{\Gamma_S^2+\Gamma_L^2}{8} & \frac{p}{q} \cdot \left(\frac{m_S^2-m_L^2}{2} + \frac{\Gamma_S^2-\Gamma_L^2}{8} \right) \\ \frac{q}{p} \cdot \left(\frac{m_S^2-m_L^2}{2} + \frac{\Gamma_S^2-\Gamma_L^2}{8} \right) & \frac{m_S^2+m_L^2}{2} + \frac{\Gamma_S^2+\Gamma_L^2}{8} \end{pmatrix} \begin{pmatrix} \Re_1 \\ \Re_2 \end{pmatrix} - \begin{pmatrix} \frac{\Gamma_S+\Gamma_L}{2} & \frac{p}{q} \cdot \frac{\Gamma_S-\Gamma_L}{2} \\ \frac{q}{p} \cdot \frac{\Gamma_S-\Gamma_L}{2} & \frac{\Gamma_S+\Gamma_L}{2} \end{pmatrix} \begin{pmatrix} \dot{\Re}_1 \\ \dot{\Re}_2 \end{pmatrix}. \quad (41)$$

With CP and T violation, i. e. $p/q \neq 1$, the differential equation for the real parts exhibits the same symmetry properties as the Schrödinger equation; the diagonal matrix elements are equal, the off-diagonal elements are different.

Acknowledgments

We are grateful to Rolf Musch and Helmut Maier in the mechanical workshop of the former Institut für Hochenergiephysik at Heidelberg for the construction of our pendulum pair, and to Christian Herdt for the construction drawing. We also thank Michael Kobel, Karlheinz Meier, and Otto Nachtmann for support and fruitful discussions, Hans-Georg Siebig, Harald Schubert, and Daniel Stegen for their help in producing the video clips, and Ernest Henley, Andrzej Buras, Svjetlana Fajfer, and Barbara Schrempp for their encouragements to publish this article.

References

- [1] B. Winstein, “CP Violation”, Festi-Val – Festschrift for Val Telegdi, edited by K. Winter, Elsevier Amsterdam, p. 245 - 265 (1988)
- [2] H. Albrecht et al. (ARGUS), “Observation of $B^0\bar{B}^0$ Mixing”, Phys. Lett. B 192, 245 - 252 (1987)
- [3] M. Gell-Mann and A. Pais, “Behavior of Neutral Particles under Charge Conjugation”, Phys. Rev. 97, 1387 - 1389 (1955)
- [4] M. Baldo-Ceolin et al., “Hyperfragments Produced by K^0 Mesons from K^+ Charge Exchange”, Phys. Rev. 112, 2118 - 2121 (1958)
- [5] F. S. Crawford et al., “Evidence for the Transition of a K^0 into a \bar{K}^0 Meson”, Phys. Rev. 113, 1601 - 1604 (1959)
- [6] See supplementary material in <http://iktp.tu-dresden.de/~schubert/pendula/links.html>
- [7] K. Nakamura et al. (Particle Data Group), “Review of Particle Physics”, J. Phys. G 37, 075021, 1422 pages (2010)
- [8] D. Asner et al. (HFAG), “Averages of b-hadron, c-hadron, and τ -lepton Properties”, arXiv:1010.1589v2, 288 pages (2011)

- [9] C. Albajar et al. (UA1), “Search for $B^0\bar{B}^0$ Oscillations at the CERN Proton-Antiproton Collider”, Phys. Lett. B 186, 247 - 254 (1987)
- [10] A. Abulencia et al. (CDF), “Measurement of the $B_s^0\bar{B}_s^0$ Oscillation Frequency”, Phys. Rev. Lett. 97, 062003, 7 pages (2006)
- [11] V. M. Abazov et al. (D0), “Direct Limits on the B_s^0 Oscillation Frequency”, Phys. Rev. Lett. 97, 021802, 7 pages (2006)
- [12] B. Aubert et al. (BABAR), “Evidence for $D^0\bar{D}^0$ Mixing”, Phys. Rev. Lett. 98, 211802, 6 pages (2007)
- [13] M. Starič et al. (BELLE), “Evidence for $D^0\bar{D}^0$ Mixing”, Phys. Rev. Lett. 98, 211803, 6 pages (2007)
- [14] J. H. Christenson et al., “Evidence for the 2π Decay of the K^0_2 Meson”, Phys. Rev. Lett. 13, 138 - 140 (1964)
- [15] G. C. Branco, L. Lavoura and J. P. Silva, “CP Violation”, 511 pages, Oxford University Press 1999
- [16] R. Jacob and R. G. Sachs, “Mass and Lifetime of Unstable Particles”, Phys. Rev. 121, 350 - 356 (1961)
- [17] R. P. Feynman, R. B. Leighton and M. Sands, “The Feynman Lectures on Physics” Vol. III, Addison-Wesley Publishing 1966
- [18] V. F. Weisskopf and E. P. Wigner, “Berechnung der natürlichen Linienbreite auf Grund der Diracschen Lichttheorie”, Z. Phys. 63, 54 -73 (1930) and “Über die natürliche Linienbreite in der Strahlung des harmonischen Oszillators”, Z. Phys. 65, 18 -29 (1930)
- [19] R. G. Sachs, “Interference Phenomena of Neutral K Mesons”, Annals of Physics 22, 239 - 262 (1963)
- [20] K. R. Schubert et al., “The Phase of η_{00} and the Invariances CPT and T”, Phys. Lett. 31 B, 662 - 665 (1970)
- [21] A. Angelopoulos et al. (CLEAR), “First direct observation of time-reversal non-invariance in the neutral-kaon system”, Phys. Lett. B 444, 43 - 51 (1998)
- [22] M. Fidecaro and H.-J. Gerber, “The fundamental symmetries in the neutral kaon system – a pedagogical choice”, Rep. Prog. Phys. 69, 1713 - 1770 (2006)
- [23] V. A. Kostelecky and A. Roberts, “Analogue models for T and CPT violation in neutral-meson oscillations”, Phys. Rev. D 63, 096002, 8 pages (2001)
- [24] J. L. Rosner, “Tabletop time-reversal violation”, Am. J. Phys. 64, 982 - 985 (1996)
- [25] J. L. Rosner and S. A. Slezak, “Classical illustrations of CP violation in kaon decays”, Am. J. Phys. 69, 44 - 49 (2001)
- [26] M. Caruso, H. Fanchiotti, and C. A. Garcia Canal, “Equivalence between classical and quantum dynamics. Neutral Kaons and electric circuits”, Annals of Physics 326, 2717 - 2736 (2011)